HADRON PHYSICS AND THE STRUCTURE OF NEUTRON STARS*)

Marek Kutschera

H. Niewodniczański Institute of Nuclear Physics
ul. Radzikowskiego 152, 31-342 Kraków, Poland

Abstract:

The equation of state of hadronic matter in neutron stars is briefly reviewed. Uncertainties regarding the stiffness and composition of hadronic matter are discussed. Importance of poorly known short range interactions of nucleons and hyperons is emphasized. Condensation of meson fields and the role of subhadronic degrees of freedom is considered. Empirical constraints on the equation of state emerging from observations of neutron stars are discussed. The nature of the remnant of SN1987A is considered.

1. Introduction

Neutron stars are the final stage of evolution of massive stars, $M > 8M_{\odot}$. They are born in supernova explosions which terminate hydrostatic evolution when heavy elements up to iron are synthesized in the core. When the mass of still growing iron core reaches the Chandrasekhar limit, the core looses stability and collapses to a neutron star. It is an open question what is the maximum mass of stars which leave neutron star after the core collapse. I shall briefly mention some recent ideas regarding this problem.

The main subject of this lecture is the equation of state (EOS) of hadronic matter which determines properties of neutron stars, in particular their internal structure. Before discussing in some detail the physics governing the EOS, I first review the observational parameters of neutron stars. Then I discuss currently considered possibilities regarding the nature of the neutron star EOS. In the last section the empirical constraints on the

*) Lecture given at the Meeting of Astrophysics Commission of Polish Academy of Arts and Sciences, Cracow, June 1996.

EOS are discussed. As particularly relevant, the nature of the remnant of SN1987A is discussed.

2. Empirical parameters of neutron stars

Neutron stars have very small radii, on order of $10km$, and cool rather quickly after birth in supernova explosion. These are principal reasons making the flux of thermal photons emitted by neutron stars practically invisible. Only young neutron stars which are sufficiently hot radiate X-ray flux which can be registered by satellite-born detectors.

Isolated neutron stars which rotate fast enough and possess strong magnetic field are observed as radio pulsars. At present $\sim$ 1000 pulsars are known and this number continuously increases. Neutron stars are also found in binaries. These accreting matter from the companion are observed as X-ray pulsars, when they have strong magnetic field, or as X-ray bursters in case of weak magnetic field. Of particular importance are binary pulsars with the companion neutron star as they allow one to measure precisely the neutron star masses. At present six such double neutron star binaries are known.

Physical parameters of neutron stars most relevant to constraining the EOS are the mass, the radius, the surface temperature and the age. Simultaneous determination of all these parameters would very tightly constrain the neutron star EOS. Unfortunately, these parameters are not easily accessible to observations.

Period of rotation and the magnetic field of pulsars could also provide important information about the internal structure of the stars. In particular, pulsar timing is a powerful means of probing neutron stars.

2.1 NEUTRON STAR MASSES

Presently, masses of about 20 neutron stars in binary systems are determined. Among them are six double neutron star binaries, PSR B1913+16 [1], PSR B1534+12 [2], PSR B2303+46 [3], PSR B2127+11C [4], PSR B1820-11 [5] and PSR J1518+4904 [6]. For three of them, PSR B1913+16, PSR B1534+12 and PSR B2127+11C, precise measurements of mass of both neutron stars are available. The masses are found to be $M_1 = 1.44M_\odot$ and $M_2 = 1.39M_\odot$ (PSR B1913+16), $M_1 = 1.34M_\odot$ and $M_2 = 1.34M_\odot$ (PSR B1534+12) and $M_1 = 1.35M_\odot$ and $M_2 = 1.36M_\odot$ (PSR B2127+11C). All masses lie in a rather narrow interval, $1.3M_\odot < M < 1.5M_\odot$. Masses of neutron stars in X-ray pulsars are also consistent with these values although are measured less accurately. The measured masses

of neutron stars apparently do not exceed the maximum mass which is about $1.5M_{\odot}$. We shall discuss possible implications of this upper limit in the last section.

2.2 NEUTRON STAR RADII

Radii of neutron stars are not directly observable. One can infer, however, some plausible values from model calculations of X-ray bursters which are of the order of $10km$.

2.3 SURFACE TEMPERATURE OF NEUTRON STARS

The X-ray flux from about 14 pulsars has been detected [7]. The spectrum of photons is more difficult to obtain. If measured, it is often not consistent with the thermal emission but is rather dominated by hard component due to magnetospheric activity. Only for four pulsars, PSR 0833-45 (Vela), PSR 0630+18 (Geminga), PSR 0656+14 and PSR 1055-52, softer blackbody component corresponding to surface thermal emission is determined.

2.4 THE AGE OF PULSARS

Pulsar ages are estimated by measuring their spin down rates. Pulsars spin down due to conversion of rotational energy into radiation. A simple spin down relation is assumed, $\dot{\nu} = K\nu^n$, where ν is the rotation frequency, and n is the braking index. The constant K for magnetic braking is proportional to d^2/I, where d is the magnetic moment of the star and I is the moment of inertia. If the energy loss is through radiation from a dipolar magnetic field, the braking index is $n = 3$. The spin-down age of pulsar is then $\tau = -\nu/2\dot{\nu}$.

The spin-down age with $n = 3$ is commonly used for pulsars. Its applicability, however, is questioned by recent measurement of the braking index of the Vela pulsar [8], which gives $n = 1.4 \pm 0.2$. This value implies that previous estimate of the age of Vela pulsar should increase by a factor ~ 3.

2.5 MAGNETIC FIELDS OF NEUTRON STARS

Magnetic fields of radio pulsars are inferred from the spin down relation assuming dipolar magnetic field. A striking feature is the bimodal distribution of pulsar magnetic fields. Usual pulsars have strong magnetic field, $B \sim 10^{12} - 10^{13}G$, whereas millisecond pulsars possess much weaker fields, $B \sim 10^8 - 10^9G$. For some X-ray pulsars the magnetic field is measured directly, by observation of absorption features interpreted as cyclotron

lines [9]. The values are in the range found for normal pulsars. It should be noted that neutron stars in the X-ray bursters have, if any, still weaker fields, $B < 10^8 G$.

Magnetic field of neutron stars could also serve as a probe of the neutron star EOS if its presence is determined by the properties of dense matter. The bimodal distribution of pulsar magnetic fields strongly suggests existence of a magnetic phase transition in neutron star matter [9]. There is a possibility, however, that some component of the magnetic field of a neutron star is inherited from the progenitor.

3. The EOS and structure of neutron stars

Before turning to the structure of neutron stars, let us make a more general remark as to the place of neutron stars among stable astrophysical objects which include planets, normal stars, white dwarfs and neutron stars. These four types of stable objects differ in the nature of material whose pressure supports them. There are, however, striking similarities as to the physical nature of the pressure between normal stars and white dwarfs, on one hand, and between planets and neutron stars, on the other hand. In the former case, the source of pressure is, respectively, the kinetic energy of thermal plasma and degenerate electron gas, whereas in the latter case the source of pressure is the interaction energy of, respectively, atoms and hadrons.

The EOS for both plasma and the electron gas is that of an ideal gas with Boltzmann and Fermi statistics, respectively. Pressure as a function of density and temperature is $p \sim \rho k_B T$, for plasma, and $p \sim \rho^{5/3}$ for electron gas. Simplicity of these formulae is due to the fact that the contribution of Coulomb interactions is dominated by much higher kinetic energies. The situation is opposite for condensed atomic matter in planets and condensed hadronic matter in neutron stars. In both systems, the interaction energy between particles dominates, with kinetic energy playing a lesser role. This makes calculation of the EOS a rather difficult task. For atomic matter, the interactions are in principle known and problems with calculating the EOS are mainly of technical nature. For condensed hadronic matter in neutron stars the situation is more challenging. The relevant interactions between hadrons in dense matter are only roughly known, a fact which is reflected in large uncertainty of the neutron star EOS.

3.1 HADRONIC MATTER OF THE CORE OF NEUTRON STARS

For physically relevant neutron stars with $M \sim 1.4 M_\odot$ the core comprises most of

the mass. The neutron star core is the interior part of the neutron star, below the crust, with densities exceeding the nuclear saturation density, $n_0 \approx 0.16 fm^{-3}$. Properties of the neutron star crust matter will not be considered here. The crust is composed of a crystal, which is similar to that in white dwarfs. In the inner crust neutrons gradually fill in the space between nuclei.

The material, from which the neutron star core is built of, is condensed hadronic matter, essentially in the ground state. Just below the crust, the core matter is composed mainly of neutrons with some admixture of protons, electrons and muons. This matter is condensed since the Fermi energy of electrons is much higher than the thermal energy, $E_F >> k_B T$. Thermal energy of particles in the neutron star is below $1MeV$, except of first few minutes after formation. The temperature of a newly born neutron star is $k_B T \sim 30MeV$. The star cools to $k_B T \sim 1MeV$ in a few minutes. The electron Fermi energy in the core is $E_F \sim 100MeV$.

Weak interactions ensure that the neutron star matter relaxes to β-equilibrium with neutron, proton and electron chemical potentials satisfying the condition

$$\mu_N = \mu_P + \mu_e. \tag{1}$$

When the electron chemical potential exceeds the muon rest mass, $\mu_e \geq m_\mu = 106MeV$, muons appear in the matter with the chemical potential $\mu_\mu = \mu_e$.

The neutron star matter is locally charge neutral, with the lepton (electrons + muons) density equal to the proton density,

$$n_e + n_\mu = n_P. \tag{2}$$

3.1.1 Neutron star matter at density n_0

Properties of neutron star matter of saturation density can be inferred from empirical parameters of nuclear matter which are obtained from nuclear mass formulae. The empirical value of nuclear symmetry energy, $E_s = 31 \pm 4MeV$ allows one to fix the proton fraction by using Eq.(1) and (2). The proton fraction, $x = n_P/n$, of β-stable nucleon matter of saturation density is

$$x(n_0) \approx 0.05. \tag{3}$$

The surface layer of the neutron star core, of density $n_0 \approx 0.16 fm^{-3}$, is the only part of the core whose composition is determined quasi-empirically. The value of the proton fraction, $\sim 5\%$, is known with accuracy determined entirely by the empirical error of the nuclear symmetry energy.

3.1.2 Neutron star matter beyond the saturation density

Investigation of deeper layers of the neutron star requires extrapolation of hadronic matter properties away from empirically accessible domain. The lack of sufficient knowledge of hadronic interactions at short distances makes this extrapolation uncertain.

To obtain properties of neutron star matter at higher densities, $n > n_0$, one has to employ a model of nucleon (hadronic) interactions which allows one to calculate the energy density of neutron star matter, ϵ, as a function of baryon density, n, $\epsilon \equiv \epsilon(n)$.

The pressure as a function of mass density, $p \equiv p(\rho)$, a relation referred to as the EOS, is determined by the energy density,

$$\epsilon(n) = \epsilon_{kin} + \epsilon_{int}, \tag{4}$$

where the kinetic energy density is

$$\epsilon_{kin} = \frac{2}{(2\pi)^3}[\int_0^{k_N} d^3k\sqrt{k^2 + m_N^2} + \int_0^{k_P} d^3k\sqrt{k^2 + m_P^2}]. \tag{5}$$

Here we use such units that $\hbar = c = 1$ and the mass density, corresponding to baryon density n, is $\rho(n) \equiv \epsilon(n)$. Pressure is $p = n^2\partial(\epsilon/n)/\partial n$.

Insufficient knowledge of hadronic interactions results in uncertainty of the interaction energy density, $\epsilon_{int}(n)$, which grows with increasing density. Various model calculations give predictions which span quite a wide range. Discrepancy of energy per particle for various EOS's exceeds a factor of 2 at the same baryon density. This translates into still higher discrepancy of pressure at a given mass density.

Astrophysical implications of such an uncertainty in the EOS can be best illustrated on the plot of the density profile of a neutron star of fixed mass $M = 1.4M_\odot$. As one can see in Fig.1, various EOS's give the radius of the star between $7km$ and $15km$. The radius of the neutron star is thus known with a 50% uncertainty. Also, as discussed below, considerable uncertainty exists as far as the internal structure of the star is concerned.

The uncertainty of the EOS affects our knowledge of the fundamental quantity of neutron star physics, the maximum mass of neutron star. Various EOS's give values in

the range $1.5M_\odot \leq M_{max} \leq 2.8M_\odot$. The measured masses of neutron stars require that the maximum mass for any EOS is $M_{max} > 1.44M_\odot$.

We now turn to address the question of hadronic interactions and their influence on the neutron star EOS.

3.2 HADRON INTERACTIONS AND THE EOS

The decisive factor for deriving the EOS of neutron star matter for densities $n \leq 3n_0$ is the interaction of nucleons. According to the theory of strong interactions, the Quantum Chromodynamics, the nucleon-nucleon interaction is some residual interaction between composite objects, whose structure is determined by the primary QCD interactions. Nucleon interactions are not derivable at present from the underlying theory. In this situation one must resort to phenomenological methods.

For calculating the neutron star EOS two main approaches are used. In the first approach which is purely phenomenological, the nucleon-nucleon interaction is parametrized in the form of a nonrelativistic potential v_{NN}. This potential is fit to reproduce the scattering data and the properties of the deuteron [10]. The second approach is based on one-boson exchange (OBE) model of nucleon scattering. The scattering amplitude is calculated assuming the exchange of the lowest mesons, whose coupling to nucleons is adjusted to fit the data [11]. Usually a simple Yukawa coupling of meson fields to nucleons is used.

EOS's obtained in both approaches differ considerably. In fact one obtains two distinct classes of EOS depending on the way in which the nucleon-nucleon interaction is constructed.

The energy per particle as a function of density,

$$E(n) = \frac{1}{n}(\epsilon_{kin} + \epsilon_{int}), \tag{6}$$

in either case is obtained by solving many-body theory with a given model interaction.

Any realistic EOS should reproduce empirical parameters of nuclear matter, which include the saturation density, $n_0 = 0.16 \pm 0.015 fm^{-3}$, the binding energy, $E(n_0) - m = -16 \pm 0.2MeV$, the compressibility modulus, $K_V = 220 \pm 30MeV$ and the symmetry energy, $E_s = 31 \pm 4MeV$.

Despite the fact that realistic nuclear interactions reproduce the above saturation properties, they give different predictions at higher densities. Of particular importance

for neutron star physics are such high density properties of the EOS as the stiffness and the proton content. One can identify the components of the nuclear potential responsible for these quantities, which are, respectively, the central potential, $v_c(r)$, and the isospin potential, $v_\tau(r)$. Retaining only these components, the nucleon-nucleon potential is

$$v_{NN}(r) = v_c(r) + v_\tau \vec{\tau}_1 \vec{\tau}_2 + ... \tag{7}$$

The short-range behaviour of the central potential, $v_c(r)$, governs mainly the stiffness of the equation of state at high densities. At short distances, the nucleon potential possesses a repulsive core. The harder the core, the stiffer is the EOS.

The isospin potential, v_τ, determines the proton fraction of neutron star matter at high densities. For many phenomenological potentials, such as Reid's potential [12], Urbana v_{14} [10], Argonne v_{14} [13], the isospin potential is negative, $v_\tau < 0$, and decreases at short distances. In this case, the potential (7) between proton and neutron is more repulsive than between two neutrons. Consequently, it is energetically favourable for protons to disappear at high densities [14,15,16]. In Fig.2 we show the isospin potential $v_\tau(r)$ corresponding to some of the above interactions.

Models based on the OBE potentials, on the other hand, predict positive isospin potential, $v_\tau > 0$, which increases at short distances. In this case, the potential (7) between proton and neutron is less repulsive than that for a pair of neutrons. We thus expect an increase of the proton fraction of neutron star matter at high density.

In Fig.3 we show the proton fraction of neutron star matter for both classes of models. A general tendency is that models of dense matter based on phenomenological potentials, which have $v_\tau < 0$, predict the proton fraction of the order of a few percent which decreases at high densities [14,15,16]. Models employing the OBE interactions predict the opposite behaviour, the proton fraction monotonically increases with density [16,17]. It is obvious that one class of models is wrong, however, at present we are not able to discriminate between them. The empirical way to do so would be to device an experiment sensitive to the short range proton-neutron interaction.

3.3 NEW DEGREES OF FREEDOM

At densities above $\sim 3n_0$ one must consider possibility that new degrees of freedom appear in the system. These include heavier baryons (hyperons) and condensates of meson fields. At still higher densities a phase transition to quark matter could also occur.

3.3.1 Hyperons

Possibility that hyperons become abundant in the neutron star matter stems from the fact that at high enough density the neutron Fermi energy can exceed the rest mass of hyperon Λ, which is $m_\Lambda = 1116MeV$ and at still higher density the mass of hyperon Σ, $m_\Sigma = 1190MeV$.

The Fermi sea of a given neutral hyperon species starts to be populated at the threshold density, n_{th}, when the neutron chemical potential for the first time becomes equal to the hyperon chemical potential in the neutron star matter,

$$\mu_N(n_{th}) = \mu_H(n_{th}, n_H = 0). \tag{8}$$

The threshold condition for negatively charged hyperons is

$$\mu_N(n_{th}) + \mu_e(n_{th}) = \mu_H(n_{th}, n_H = 0). \tag{9}$$

In these formulae the hyperon density at the threshold is $n_H = 0$.

Conditions (8) and (9) are very sensitive to interactions of the hyperon with neutrons. The hyperon chemical potential at the threshold can be written as

$$\mu_H \approx m_H + E_{int}^{NH}(n_{th}), \tag{10}$$

where the last term represents the interaction energy of a single hyperon with the neutron star matter.

Sometimes a misleading argument is used to show that hyperon component is present at high density. A simple estimate of the threshold density can be obtained if one ignores the interaction term in Eq.(10). With this assumption the condition (8) can always be satisfied at some density, as the neutron chemical potential monotonically increases with density. However, such an estimate can be meaningless, as the the interaction term cannot be neglected.

Our knowledge of hyperon interactions in high density matter is insufficient to conclude that hyperon Fermi sea is present in the neutron star matter. The strength of the hyperon-neutron interaction relative to the neutron-neutron interaction will decide whether hyperons appear in the neutron star matter or not. In terms of the short-range potentials, if the neutron-hyperon interaction is more repulsive than the neutron-neutron one,

$$v_{NH} > v_{NN}, \tag{11}$$

no hyperons appear in dense matter at any density [14]. If the opposite relation is true at short distances,

$$v_{NH} \leq v_{NN}, \tag{12}$$

there can exist a threshold density, above which the hyperons appear in the matter [18].

The situation here is analogous to that for protons discussed above where also the relative strength of proton-neutron and neutron-neutron interaction determines the proton content at high densities.

3.3.2 Meson condensates

Attractive interactions of light mesons with nucleons in the neutron star matter can lower their effective mass sufficiently enough that formation of the Bose condensate could be energetically favourable. Negatively charged mesons, π^- and K^-, can be formed when their chemical potentials become equal to the electron chemical potential,

$$\mu_{\pi^-} = \mu_e, \qquad\qquad \mu_{K^-} = \mu_e. \tag{13}$$

The meson chemical potential is the lowest eigenstate of the meson in the matter. Once the threshold condition (13) is satisfied, the lowest mode becomes macroscopically populated.

The possibility of pion condensation was extensively discussed in the literature [19]. The p-wave pion-nucleon interaction results in a spatial modulation of the condensate. Presence of the pion condensate strongly affects cooling of neutron stars. Because of additional binding, the EOS of pion condensed matter is softer.

Recently possibility of the kaon condensation in neutron star matter has been considered [20]. The kaon-nucleon interaction is mainly s-wave and the condensate is uniform [21]. Neutron star matter with kaon condensation has rather soft equation of state. A very interesting feature of this EOS is the fact that maximum neutron star mass calculated for cold matter, after the neutrinos trapped in the newly born neutron star are radiated away, is lower than the one with trapped neutrinos [21].

3.3.3 Quark matter

It is expected that quarks which are constituents of hadrons become liberated at high densities. The simple argument is of geometrical nature: Hadrons are extended objects

which at high densities must overlap deconfining the quarks. The deconfinement density is strongly model dependent. Estimates give the deconfinement phase transition in the range $4-10n_0$. Maximum quark core corresponds to the continuous phase transition from nucleon matter to quark matter [22].

This picture of hadron to quark phase transition may be somewhat naive in view of recent lattice QCD calculations. At high densities and/or temperatures QCD predicts restoration of chiral symmetry. It is important for our picture of dense matter in neutron star which transition occurs first. Common assumption is that the deconfinement occurs at lower densities than the restoration of chiral symmetry [23,24]. Quark matter relevant to neutron stars with broken chiral symmetry can develop spatially modulated chiral condensate [23,24].

Recently a different scenario of hadron to quark transition has been considered by G. Brown et al.[25] who propose that at high temperatures and/or densities hadrons become first massless and the color deconfinement occurs at much higher temperature and/or density.

3.4 UNCERTAINTY OF EOS AND THE STRUCTURE OF NEUTRON STARS

Theoretical models of dense matter discussed above constrain weakly stiffness of the EOS which is the most important property of the neutron star EOS.

3.4.1 Stiffness of EOS and the maximum mass of neutron star

Stiffness is a global property of the EOS which measures how fast the pressure increases with increasing mass density. In Sect.3.2 we discussed the influence of the repulsive core in nucleon-nucleon potential on the stiffness. Also presence of hyperons and meson condensates in the neutron star matter affects stiffness of EOS, which becomes softer. A similar softening of the EOS occurs when the quark phase is present.

The stiffness of the neutron star EOS determines the value of the maximum mass of neutron star, which plays the role of Chandrasekhar mass for neutron stars. A general rule is that the maximum mass for soft EOS is lower than that for stiffer EOS, $M_{max}^{soft} < M_{max}^{stiff}$. Softest EOS's, still compatible with measurements of neutron star masses, give $M_{max} \approx 1.5 M_\odot$. Stiffest realistic EOS's predict $M_{max} \approx 2.8 M_\odot$.

3.4.2 Structure of neutron stars

Internal structure of the neutron star depends on its mass. Here we consider physically relevant neutron star of mass $M = 1.4M_{\odot}$. For a neutron star of a given mass the radius for soft EOS is smaller than for stiff EOS, $R^{soft} < R^{stiff}$. The central density of this star is higher in case of soft EOS than for stiff EOS, $n_c^{soft} > n_c^{stiff}$. Also, the crust thickness for soft EOS is lower than for stiff EOS.

The proton fraction of neutron star matter has important consequences for magnetic properties. If proton fraction is low, $x \sim 0.05$, and does not increase with density, it is likely that protons become localized [26,27] at high densities. Localized protons can form a crystal lattice [28]. Neutron star matter with localized protons is unstable with respect to spontaneous polarization [29]. This phase of neutron star matter possesses permanent magnetization [29,30] and can contribute to the magnetic moment of the neutron star. The same proton-neutron interactions which are responsible for low proton fraction of uniform matter, tend to separate protons and neutrons [31] and localize the protons.

When proton fraction increases with density, it can exceed the threshold for direct URCA process, $x_{URCA} \approx 0.11$. This would strongly enhance the cooling of neutron stars.

Available EOS's allow us to construct various scenarios of the internal structure of the neutron star core. Let us briefly describe two consistent possibilities, corresponding to two classes of neutron star EOS's, considered in Sect.3.2.

The models of EOS based on phenomenological potentials, which predict low proton fraction, suggest the following structure. Below the solid crust there is a layer of normal uniform matter, with proton fraction $\sim 5\%$. At some deeper level, where the localization density is exceeded, proton localization occurs and neutron star matter acquires magnetization [30]. There exist thus an inner shell which is magnetized. If the transition to quark matter occurs at neutron star densities, there could exist a quark core surrounding the center of the star.

In this scenario it is unlikely that hyperons exist in the neutron star matter as they are expected to interact with neutrons in a similar way as do the protons. Also, the chemical potential of electrons decreases with density making kaon condensation rather unlikely.

The class of EOS's based on OBE potentials or relativistic mean field theory predicts quite a different internal structure of the neutron star. The layer, just below the crust, is the same as for phenomenological models. It is normal uniform matter containing some 5% of protons. However, in deeper layers the proton fraction increases and hyperons appear in the neutron star matter. In still deeper layers kaon condensate is present. It is likely in

this scenario that the chiral symmetry is restored in the center of the star. Neutron star matter near the center is composed of a mixture of nearly massless hadrons.

There exist a variety of neutron star EOS's derived by astrophysicists. Clearly, some of them are incompatible with one another. Below we discuss how the neutron star EOS could be constrained empirically.

4. Empirical constraints on the neutron star EOS

The EOS of neutron star matter at high densities is not at present constrained sufficiently by theory to allow conclusive statements as to the internal structure of neutron stars. In view of weakness of theoretical constraints it is urgent to empirically constrain the EOS.

4.1 LABORATORY EXPERIMENTS

Scattering of heavy ions, which is the only laboratory way to study properties of dense matter, does not probe directly the EOS relevant to neutron stars. In nuclear collisions highly excited hadronic matter is formed which decays quickly into stable particles. One should perform extrapolations in order to obtain ground state properties from these data which would involve considerable uncertainty. However, many important informations regarding the neutron star EOS can be inferred from scattering data. In particular, interactions of hyperons formed in nuclear collisions with nucleons in dense fireball can be studied. Also, detection of quark-gluon plasma in heavy ion collisions could give valuable information about energy density range in which one can expect deconfinement transition in neutron star matter.

4.2 OBSERVATIONS OF NEUTRON STARS

Discovery of a sub-millisecond pulsar would severely constrain the EOS. Unfortunately, reported observations of 0.5 ms pulsar in the SN1987A remnant [32] turned out to be erroneous. The fastest millisecond pulsar of period 1.56 ms does not exclude any realistic EOS.

4.2.1 X-rays from rotation-powered pulsars

Observation of thermal flux of photons from a pulsar, whose age can be estimated, can provide information how fast the neutron star cools. Probing the cooling curve of

neutron stars is considered to be the most profitable method to learn about the internal composition of neutron stars.

Recent observations of thermal X-ray flux from four pulsars give promise that in near future the cooling curve will be empirically constrained. The main objective of these observations is to discriminate between fast and slow cooling mechanisms.

Slow cooling proceeds mainly through the modified URCA process,

$$n + n \to n + p + e^- + \bar{\nu}_e, \qquad n + p + e^- \to n + n + \nu_e.$$

It is the dominating mechanism of standard cooling scenario for neutron stars whose proton content is below the critical value, $x < x_{URCA} \approx 0.11$.

If the proton content exceeds the critical value, $x > x_{URCA}$, or there exist kaon (or pion) condensate in neutron star matter, cooling proceeds through direct URCA process,

$$n \to p + e^- + \bar{\nu}_e, \qquad p + e^- \to n + \nu_e.$$

This cooling mechanism is much faster, and, correspondingly, the temperature of the neutron star is lower than for modified URCA.

Recent comparison of the X-ray luminosities of four pulsars [33] is not conclusive, but the observational data are somewhat closer to the standard cooling curve.

4.2.2 Remnant of SN1987A

Detection of neutrino flux associated with optical observation of supernova SN1987A was the best confirmation of the theory of neutron star formation in supernova Type II explosions. Present observations of the light curve of the remnant of SN1987A do not confirm existence of the neutron star. Continuously decreasing luminosity of the remnant of SN1987A suggests that Crab-like pulsar does not exist in the remnant. Also, no hot X-ray source is observed. This lack of signature of neutron star led some authors [34] to speculate that the neutron star formed initially in SN1987A was in a metastable state and subsequently collapsed to black hole. Presence of a black hole in SN1987A would strongly constrain the neutron star EOS.

Scenario of black hole formation in SN1987A is as follows. The progenitor star of SN1987A is known to have mass $18M_\odot < M < 20M_\odot$. Evolutionary calculations show [35] that this star developed an iron core of mass $\sim 1.6M_\odot$ which collapsed to form hot neutron star. This neutron star existed at least for $\sim 10s$, a period when the neutrino

emission took place. After radiating away the trapped neutrinos the neutron star has lost stability and collapsed to black hole.

This scenario requires that the EOS has some unique features. The maximum mass corresponding to the hot neutron star matter, with trapped neutrinos, M_{max}^{hot}, has to be higher than the mass $M_{ns} \sim 1.6 M_{\odot}$ of the neutron star formed in the collapse of SN1987A, $M_{ns} < M_{max}^{hot}$. After emitting neutrinos the neutron star looses stability which requires that its mass is higher than the maximum mass of a neutron star corresponding to cold neutron star matter, $M_{max}^{cold} < M_{ns}$. The EOS with kaon condensation can meet these constraints [21], as we mentioned in Sect.3.3.2. The maximum mass for cold EOS is $M_{max}^{cold} = 1.5 M_{\odot}$.

The maximum mass of neutron star of $1.5 M_{\odot}$ explains in a natural way the cutoff observed in measured masses of neutron stars. Existence of such a limit is very surprising in view of the fact that considerable amount of material, at least a few tenths of solar mass, is expected to fall back onto newly formed neutron star after the explosion. One would expect many heavier neutron stars to be formed.

If the maximum mass of neutron star is $M_{max} = 1.5 M_{\odot}$ then one can determine maximum mass of the progenitor star, whose collapse can leave the neutron star remnant. For an isolated star this mass is about $20 M_{\odot}$. Heavier stars are expected to leave black hole remnants. The problem of formation of many low mass black holes in Galaxy is discussed in [36].

This work is partially supported by the Polish State Committee for Scientific Research (KBN), grants 2 P03D 001 09 and 2 P03B 083 08.

References

1. J. H. Taylor and J. M. Weisberg, Astrophys. J. **345**, 434 (1989).
2. A. Wolszczan, Nature **350**, 688 (1991).
3. S. E. Thorsett, Z. Arzoumanian, M. M. McKinnon and J. H. Taylor, Astrophys. J. **405**, L29 (1993).
4. W. T. S. Deich and S. R. Kulkarni, in *Compact Stars in Binaries*, J. van Paradijs, E. P. J. van den Heuvel and E. Kuulkers eds., Dordrecht, Kluwer (1996).
5. Z. Arzoumanian, Ph. D. thesis, Princeton Univ. (1995).
6. D. J. Nice, R. W. Sayer and J. H. Taylor, Astrophys. J. **466**, L87 (1996).
7. H. Ögelman, in *The Lives of Neutron Stars*, M. A. Alpar, U. Kiziloglu and J. van

Paradijs eds., Dordrecht, Kluwer (1995).

8. A. G. Lyne, R. S. Pritchard, F. Graham-Smith and F. Camilo, Nature **381**, 497 (1996).
9. K. Makishima, in *The Structure and Evolution of Neutron Stars*, D. Pines, R. Tamagaki and S. Tsuruta eds., Addison-Wesley (1992).
10. I. E. Lagaris and V. R. Pandharipande, Nucl. Phys. **A359**, 331, 349 (1981).
11. R. Brockmann and R. Machleidt, Phys. Rev. C **42**, 1965 (1990).
12. R. V. Reid, Ann. Phys. **50**, 411 (1968).
13. R. W. Wiringa, R. A. Smith and T. L. Ainsworth, Phys. Rev. C **29**, 1207 (1984).
14. V. R. Pandharipande and V. K. Garde, Phys. Lett. **39B**, 608 (1972).
15. R. W. Wiringa, V. Fiks and A. Fabrocini, Phys. Rev. C **38**, 1010 (1988).
16. M. Kutschera, Z. Phys. A **348**, 263 (1994).
17. K. Sumiyoshi, H. Toki and R. Brockmann, Phys. Lett. **B276**, 393 (1992).
18. N. K. Glendenning, Nucl. Phys. **A493**, 521 (1989).
19. G. E. Brown and W. Weise, Phys. Rep. **27C**, 1 (1976).
20. D. B. Kaplan and A. E. Nelson, Phys. Lett. **B175**, 57; **B179**, 409(E) (1986).
21. V. Thorsson, M. Prakash and J. M. Lattimer, Nucl. Phys. **A572**, 693 (1994).
22. M. Kutschera and A. Kotlorz, Astrophys. J. **419**, 752 (1993).
23. M. Kutschera, W. Broniowski and A. Kotlorz, Phys. Lett. **B237**, 159 (1990).
24. M. Kutschera, W. Broniowski and A. Kotlorz, Nucl. Phys. **A516**, 566 (1990).
25. G. E. Brown, A. D. Jackson, H. A. Bethe and P. M. Pizzochero, Nucl. Phys. **A560**, 1035 (1993).
26. M. Kutschera and W. Wójcik, Acta Phys. Pol. **B21**, 823 (1990).
27. M. Kutschera and W. Wójcik, Phys. Rev. C **47**, 1077 (1993).
28. M. Kutschera and W. Wójcik, Nucl. Phys. **A581**, 706 (1994).
29. M. Kutschera and W. Wójcik, Phys. Lett. **B223**, 1 (1989).
30. M. Kutschera and W. Wójcik, Acta Phys. Pol. **B23**, 947 (1992).
31. M. Kutschera, Phys. Lett. **B340**, 1 (1994).
32. C. Kristian, et al., Nature **338**, 234 (1989).
33. Ch. Schaab, F. Weber, M. K. Weigel and N. K. Glendenning, astro-ph/9603142.
34. G. E. Brown, S. W. Bruenn and J. C. Wheeler, Comments Astrophys. **16**, 153 (1992).
35. S. E. Woosley and F. X. Timmes, astro-ph/9605121.
36. G. E. Brown, J. C. Weingarten and R. A. M. J. Wijers, astro-ph/9505092.

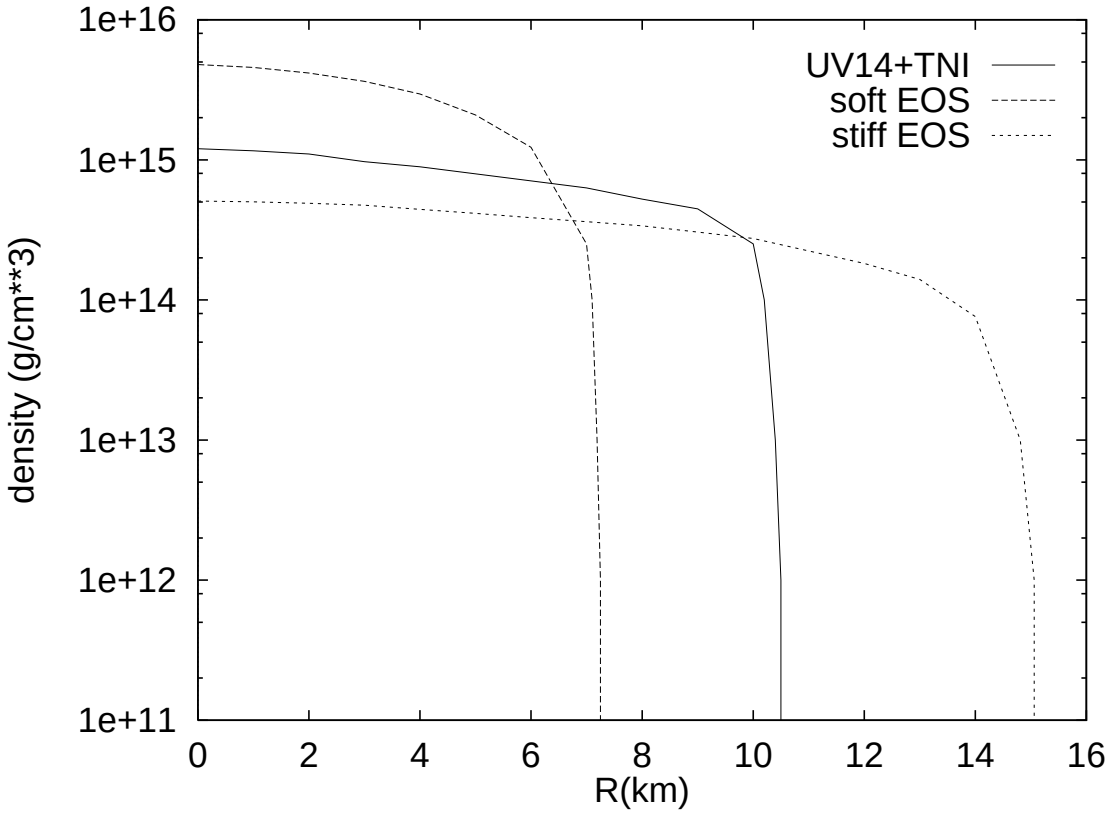

Fig.1

Density profile of $1.4M_{\odot}$ neutron star for typical soft, medium, and stiff equations of state.

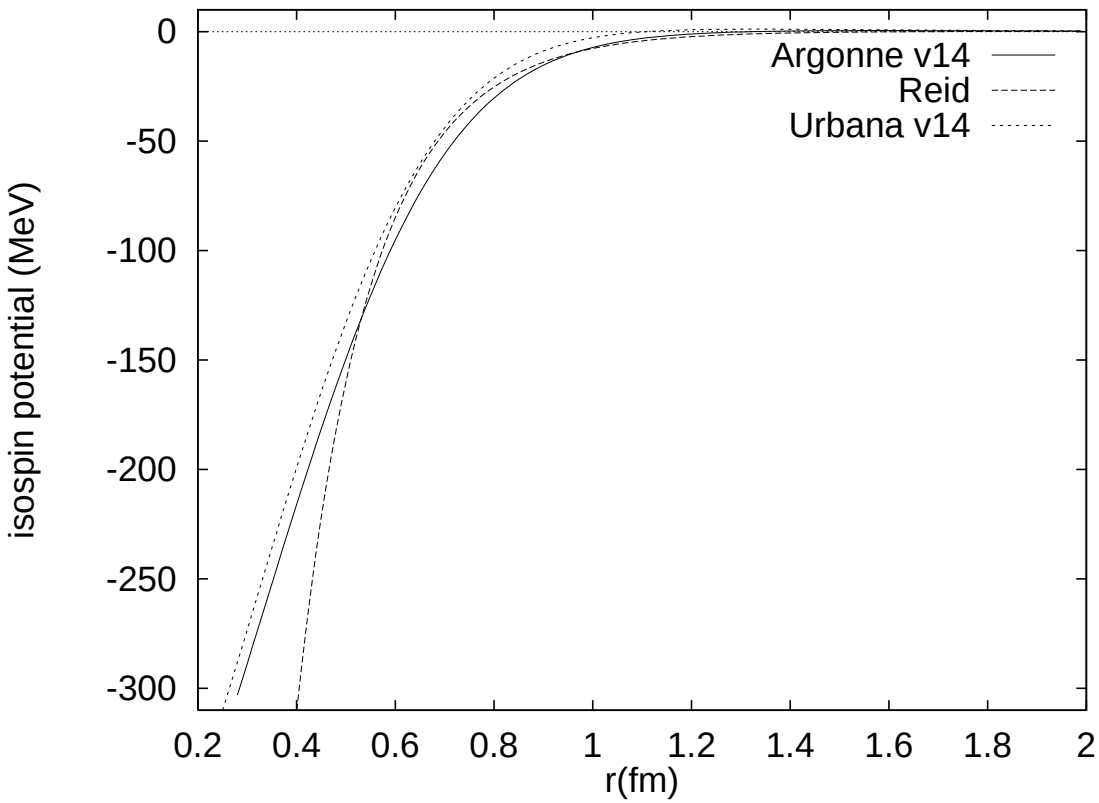

Fig.2

The isospin potential of Reid, Argonne v_{14}, and Urbana v_{14} nuclear potentials.

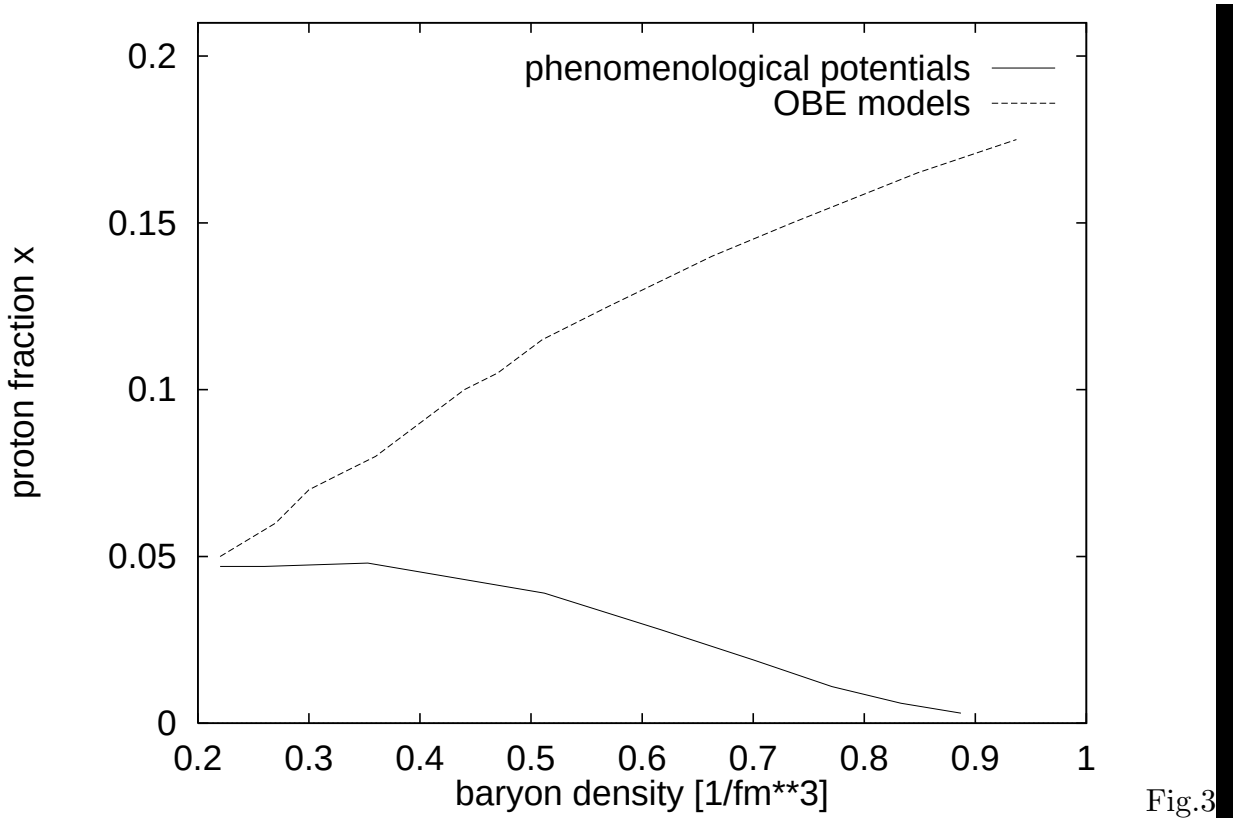

Fig.3

Proton fraction as a function of density for OBE models and for phenomenological models with isospin potential $v_\tau < 0$.